A Preliminary Study on the Global Land Annual Precipitation Associated with ENSO during 1948–2000

P4 A

Shi Neng (施 能)①, Chen Luwen (陈绿文), and Xia Dongdong (夏冬冬)

Nanjing Institute of Meteorology, Nanjing 210044

(Received September 10, 2001; revised May 10, 2002)

ABSTRACT

The global land monthly precipitation data (PREC / L) are used to investigate the relation between the global land annual precipitation and ENSO during 1948–2000, and the results of composite analysis are tested with Monte Carlo simulations. Results indicate that the global land annual precipitation was significantly reduced in large scale areas in warm event years: the areas were the equatorial West Pacific, North China; equatorial Central America; North Bengal Bay and Nepal; East Australia; West India and South Pakistan; the district east of the Lena River; West Europe; and Wilkes Land of Antarctica. In contrast to this, the areas where precipitation increased in warm event years were less, and mainly in Chile and Argentina of South America; Somali, Kenya, and Tanzania of East Africa; Turkey, Iraq, and Iran of the Middle East; Libya and Nigeria of North Africa; Namibia of Southwest Africa; and Botswana and Zimbabwe of southern Africa. Statistical tests show that in warm event years, the area where the land annual precipitation was reduced was larger than the area where the annual precipitation increased, and the reduction in precipitation was more significant than the increase. The results in this paper are compared with previous studies. It is also pointed out that the interdecadal change of ENSO had no significant effect on the interdecadal variation of precipitation in the above regions. However, the warm events of El Nino affected the droughts in East Australia and North China more after the 1980s than before.

Key words: global precipitation, ENSO, global drought / flood, interdecadal change

1. Introduction

Precipitation is an important component of climate. Studies on the climatic changes of global precipitation in the past were too seldom compared with those of global temperature due to the limitation of global precipitation data. Existing studies (Rasmusson and Carpenter 1982; Ropelewsi and Halpert 1987; Bradley et al. 1987a; Lau and Sheu 1988, 1991; Nicholson et al. 2000; Hulme 1992; Noel and Changnon 1998) showed that the large–scale anomalies of global precipitation were associated with ENSO. It was generally held that ENSO events were associated with droughts in tropical continents. However, these studies do not contain ENSO events after the 1980s. In order to avoid the influence of an exceptionally strong ENSO event on results, Ropelewsi and Halpert (1987) deliberately removed the strong ENSO event of 1982 / 83. Hulme (1992) pointed out that the reduction in the global precipitation in 1951–1980 was related to ENSO events over the same period. Bradley et al. (1987a, b) studied ENSO events before 1976. They conducted a composite analysis of the zonal belt mean precipitation over Africa between 0° and 30°N, North America, and Southeast Asia for

①E-mail: Shin@public1.ptt.js.cn

the El Niño and La Niña events from 1884–1976 and pointed out that in warm events, the zonally averaged precipitation over the northern tropical area was inclined to a reduction, and the anomaly of precipitation over the African continent was the weakest among the three. The amplitude of anomalies as well as the sign of signals in some circumstances varied greatly with longitude. Bradley et al. also pointed out that the precipitation of the equatorial area in 1983 was very small (the lowest among the precipitation records in 1900–1983), which resulted from the influence of the 1982 / 83 ENSO event. Lau and Sheu (1991) studied the relation between the global precipitation at 155 observational stations and ENSO from 1901 to 1980 using the EOF method and gave globally sequenced drought / flood areas. Hulme (1992) investigated the relations of the global mean precipitation and northern and southern tropical area precipitation with ENSO (SOI) from 1951 to 1980; the correlation coefficients were 0.49, 0.33, and 0.24 respectively, indicating that the reduction in the global precipitation was correlated with ENSO events from 1951–1980. Recently, Nicholson et al (2000) studied the rainfall anomalies over West Africa during the 1997 / 98 ENSO event.

Many papers in China have studied the relation between ENSO and rainfall over China. However, all focused on the summer / autumn rainfall of China, and none involved the annual rainfall. And papers in China that which addressed the relation between ENSO and the spatial distribution of global precipitation have been rare. Although Wang and Gong (1991) divided warm / cold event years and conducted statistical tests on the time series of global mean annual rainfall before 1993, they could not reveal the influence of ENSO events on the spatial distribution of global precipitation.

As we know, the 1997 / 98 ENSO event was the strongest one in the last hundred years and the 1982 / 83 and 1991 / 92 ENSO events were also abnormally strong. It is necessary to extend research to the relation between ENSO and global rainfall in recent years. Besides, according to Wang (1994, 1995), ENSO has changed interdecadally and has become intense and frequent since 1977. It is also necessary to determine whether there are interdecadal changes in the relation between global rainfall and ENSO by using recent precipitation data.

Recently, Chen et al. (2001, 2002) reconstructed the complete global land rainfall since 1948. They denote the reconstruction of global precipitation as PREC, the land data as PREC / L, and the maritime part as PREC / O. PREC / L was finished recently and has beer extended to December 2001. Because the PREC / L data couer 53 years in total, there are enough ENSO events for us to reliably evaluate the rainfall changes during those events. Base d on the PREC / L data, this paper studies the association of ENSO with the large–scale spatial distribution of global annual precipitation, and the correlation is tested using Monte Carlo simulations. The relation of interannual anomalies of regional annual rainfall with ENSO is addressed in section 4, the relation of interdecadal anomalies of ENSO with global annual precipitation in section 5, and a summary in section 6.

2. Data and methods

2.1 *Data*

The global land monthly precipitation data (PREC / L) from 1948 to 2000, recently created and released by Chen et al. (2001), were used in this paper. These analyses are derived from gauge observations from over 17000 meteorological stations collected in the Global Historical Climatology Network (GHCN) version 2 and the Climate Anomaly Monitoring System (CAMS) data sets collected and compiled by the U.S. Climate Prediction Center (CPC). The

spatial resolution of the data is 2.5° lat. / long. from 88.75°S to 88.75°N, with 10368 grid points in total and 4390 grid points over land. Optimum interpolation, rigorous checking and quality control were used in the creation of the data, and Chen et al. (2002) has elaborated its fine properties. The data are originally given in units of 0.1 mm d^{-1}, and we summed 12 months of data to get the annual rainfall in units of mm yr^{-1}.

2.2 *Methods*

2.2.1 *Cold/ warm event years*

Up to now, there have been many methods to define ENSO events, however those definitions have led to approximately similar cold / warm event years with some differences in a few individual years, such as 1963, 1968 / 69, 1986 / 87 and so on. In this paper, weaker ENSO years were also taken into account, thus 1963 was added. Besides, based on the results of Xu and Chan (2001), Trenberth (1997), and Wang and Gong (1999), 1968 and 1986 were defined as the beginning years of the 1968 / 69 and 1986 / 87 ENSO events respectively. Also based on the latest data and the results of Li and Ding (1997), the cold / warm events after 1990 were added. Thus, there were 14 warm event years and 10 cold event years from 1948 to 2000, and their beginning years are listed in Table 1.

Table 1. Warm / cold event years from 1948 to 2000

Warm event years	1951	1953	1957	1963	1965	1968	1972	1976	1982	1986	1991	1993	1994	1997
Cold event years	1949	1954	1955	1964	1970	1973	1975	1984	1988	1998				

2.2.2 *Student's t–test*

Differences between the global land annual rainfall means of cold / warm event years from 1948 to 2000 were examined by means of the Student's t–test. The calculation of t_i is given by

$$t_i = \frac{\overline{X}_{i1} - \overline{X}_{i2}}{\sqrt{\dfrac{N_1 S_{i1}^2 + N_2 S_{i2}^2}{N_1 + N_2 - 2}}} \sqrt{\frac{N_1 N_2}{N_1 + N_2}}, \qquad i = 1,2,\cdots,m, \tag{1}$$

where m= 4390 grid boxes, each representing a 2.5° × 2.5° latitude–longitude area, $\overline{X}_{i1}$ ($\overline{X}_{i2}$) is the annual rainfall mean, S_{i1}^2 (S_{i2}^2) is the variance of warm (cold) event years at the ith grid point, and $N_1 = 14$ ($N_2 = 10$) is the number of warm (cold) event years. If the absolute value of t is greater than the critical value t_α of statistic t with the $N_1 + N_2 - 2$ degrees of freedom at the α significance, then it can be statistically inferred that the influence of warm / cold events on annual rainfall is significant. The inference is significant at the $1-\alpha$ confidence level, where 0.01 or 0.05 is usually chosen for α. An anomalous area consists of at least 20 adjacent grid boxes which reach the confidence level.

2.2.3 *Monte Carlo simulation*

Although the t–test for differences of precipitation between warm and cold years may reliably assess the influence of ENSO on global annual rainfall, the computational domain consists of a great quantity of grid boxes (4390 grid boxes). Livezey and Chen (1983) pointed out

that the correlations between meteorological variable fields which consist of a great quantity grid boxes must be tested with Monte Carlo simulations. If the number of grid boxes at which the correlations are significant exceeds a certain criterion, the correlation can be considered to be reliable, otherwise it might occur by accident. The following statistical test method of Monte Carlo simulations was designed for the composite analysis of the annual rainfall fields on 4390 grid boxes. Because warm / cold event years were selected from the 53–year data, a random number generator was used to get 53 uniformly distributed random numbers. According to the numbers, the 14 warm event years and 10 cold event years were reshuffled. Then, by using the original global annual rainfall data, the t–statistic in Eq.(1) was calculated again and tested for each grid box, and the number of grid boxes locally significant at the α level was counted. This experiment was performed for a total of 1000 runs, and the warm / cold event years for each run were generally different. It was easy to determine thresholds for the 5% and 1% field significance by sequencing the respectively passed grid box numbers for all 1000 runs. The correlation thresholds of Monte Carlo simulations can only be calculated for specific data (e.g., the 53–year global annual rainfall data in this paper), which demands a vast amount of calculation.

3. Global land rainfall anomalies and ENSO

Table 2 lists the major statistical results of the t–statistic calculated using Eq.(1), showing that there are 1392 more negative–valved grid boxes than positive–valued ones (negative at 2891 grid boxes; positive at 1499 grid boxes), indicating that the mean rainfall at most stations in warm event years was reduced. Grid boxes with correlations significant at the 0.05 and 0.01 confidence levels are 545 and 212 respectively, which are greater than the correlation thresholds of Monte Carlo simulations at the 0.05 level, therefore suggesting that the influence of warm / cold events on the global annual precipitation is not by chance.

Table 2. Grid box numbers with t–statistic reaching confidence test standards and thresholds for Monte Carlo tests

	Negative grid boxes minus positive ones	0.05 (α)	0.01 (α)
Calculated values	1392	545	212
Thresholds (confidence level) for Monte Carlo simulations	1360 (95%)	489 (95%)	107 (95%)

The spatial distribution of the t–statistic is shown in Fig. 1, where it can be seen that the negative–valued areas of t (reduced rainfall in warm event years; increased rainfall in cold event years) are concentrated in the following nine areas.

D1: Equatorial West Pacific region (16.25°S–16.25°N, 96.25°–151.25°E; Fig. 2a). There are 322 grid boxes in the region, which covers Indonesia, the Philippines, and Singapore.

D2: North China (33.75°–38.75°N, 101.25°–113.75°E; 38.75°–41.25°N, 106.25°–118.25°E; 43.75°–51.25°N, 108.75°–113.75°E; Fig. 2b) contains 36 grid boxes. It is worth pointing out that the correlation coefficient between the annual rainfall values in the area from the PREC / L data and those from the 160–station rainfall data compiled by the climate center of China is 0.91 (1951–2000), indicating that the PREC / L is fairly accurate.

D3: Equatorial Central America area (6.25°S–21.25°N, 33.75°–91.25°W; Fig. 2c). It includes the south part of Mexico, Nicaragua, Panama, Colombia, and Venezuela in the north

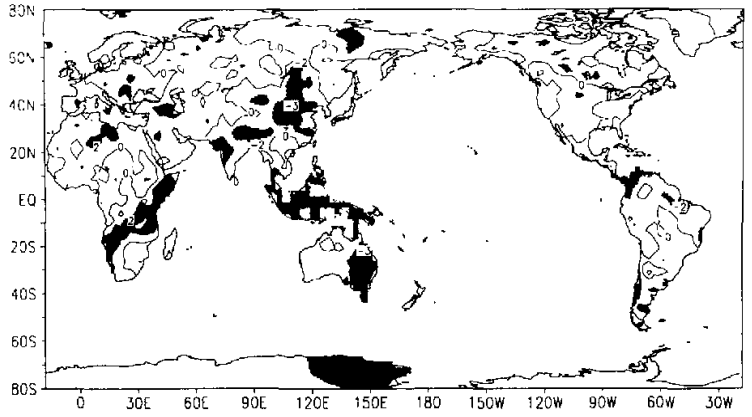

Fig. 1. The *t*-statistic of the difference of annual rainfall for cold and warm event years. Dashed lines denote negative values, and the black and gray areas denote where the correlation of annual rainfall with ENSO is significant at the 0.01 and 0.05 level respectively.

part of South America, and the region north of the Amazon, 288 grid boxes in total.

D4: North part of the Bay of Bengal and Nepal (28.75°–31.25°N, 76.25°–116.25°E; Fig. 2d). It covers 34 grid boxes.

D5: East Australia region (43.75°–21.25°S, 136.25°–153.75°E; Fig. 2e) includes 61 grid boxes.

D6: India–Pakistan region (11.25°–28.75°N, 68.25°–96.25°E; Fig. 2f) contains 96 grid boxes in West India and South Pakistan.

D7: Region east of the Lena River (63.75°–71.25°N, 133.75°–143.75°E; Fig. 2g) contains 20 grid boxes.

D8: West Europe (43.75°–51.25°N, 18.75°–31.25°E; Fig. 2h) includes 24 grid boxes.

D9: Wilks Land of Antarctica (76.25°–63.75°S; 121.25°–156.25°E; Fig. 2g) contains 44 grid boxes. The PREC/L data show that the rainfall was correlated with ENSO, however the time series of rainfall (omitted) over this area exhibits a very small variance before 1977, suggesting that the interpolated rainfall data over the Antarctic may not be reliable. Therefore the correlation in this area was not studied in greater detail.

There are 925 grid boxes in total in the above nine areas where the annual rainfall was reduced (increased) in warm (cold) event years.

Figure 3 shows the five positive-valued areas of the *t*-statitstic.

F1: Chile and Argentina of South America (48.75°–33.75°S, 68.75°–53.75°W; Fig. 3a) contain 43 grid boxes.

F2: Somalia, Kenya, and Tanzania of East Africa (11.25°–3.75°S, 23.75°–48.75°E; Fig. 3b) include 32 grid boxes.

F3: Turkey, Iraq, and Iran (21.25°–41.25°N, 38.25°–61.25°E: Fig. 3c) contain 87 grid boxes.

F4: Libya and Algeria of North Africa (21.25°–31.25°S, 3.75°–18.75°E: Fig. 3d) contain 35 grid boxes.

F5: Namibia of Southwest Africa, and Botswana, Zimbabwe, and Madagascar in Southern Africa (11.25°–26.25°S, 18.75°–58.75°E: Fig. 3e) include 83 grid boxes.

The above five positive-valued areas contain 280 grid boxes, about one third of the num-

ber of negative-valued grid boxes; thus the range of positive-valued areas is very small. Furthermore, according to Tables 3 and 4, the correlation of annual rainfall with ENSO in the positive-valued areas is far weaker than that in the negative-valued areas.

4. Interannual anomalies of regional annual precipitation and ENSO

In order to investigate the interannual variations of precipitation over anomalous areas in detail, Table 3 (4) lists the means, differences, and t-statistic values of annual rainfall for cold and warm event years over areas where the annual rainfall was low (high) in warm event years. In Table 3 (4), the drought (flood) areas are sequenced according to t-statistic values, and Fig. 3 (4) displays the temporal evolution of the normalized regionally averaged annual rainfall over the 8 drought (5 flood) areas.

According to Tables 3 and 4, and in comparison with the results of previous studies, the following points can be obtained (for convenience, D1–D8 and F1–F5 defined above are used to represent a concrete influence area of ENSO).

1) D1 is the most significant area of ENSO influence, and the negative correlation between annual rainfall and ENSO holds for all 24 years. This is consistent with results of previous qualitative studies. The circumstances of D3 are similar with D1.

2) North China was considered an insignificant area in the past. However many studies confirmed that the summer rainfall over D2 was reduced in the onset years of ENSO. This paper points out that it is a significant area of ENSO influence next to D1 in the globe, and is also a distinct drought / flood region with a large area. Fig. 2b indicates that the negative correlation holds for 24 years except for 1963. However, it is a very weak ENSO year, and was not included as an ENSO year in some papers such as Noel and Changnon (1998) or Ropelewsi and Halpert (1987).

3) The drought / flood characteristics of D5, F1, F2, and F3 are consistent with results of previous studies.

4) Indian droughts (warm event years) are not very significant (the sixth in the name list), which might be due to use of annual rainfall instead of Indian monsoon rainfall (June to September precipitation) in our calculation.

5) D4 and D8 were not included in previous studies. Our results show that, first, the annual rainfall over D4 is obviously correlated with ENSO, and second, the annual rainfall over D8 is also related with ENSO, however the correlation is weaker.

6) Using data up to 1980, Lau and Sheu (1991) concluded that North Mexico–Southern United States (California to Florida) and South China are waterlogged areas in warm event years. However, the relation is insignificant in this paper. The position of waterlogged areas of Southern Africa and Madagascar in their paper has moved northwestward (F5) in this paper. Besides, we point out that F4 is a weaker correlation area.

Table 3. Areas with reduced annual rainfall in warm event years and their averaged annual rainfall (Units: mm)

	D1	D2	D3	D4	D5	D6	D7	D8
Warm event	1729.4	319.9	1332.2	2973.5	529.9	2297.9	657.5	1596.9
Cold event	2320.2	388.8	1552.3	3318.9	667.9	2580.1	775.5	1766.7
Difference	−590.8	−68.9	−220.1	−345.4	−138.0	−282.2	−118.0	−169.8
Statistic	−8.68	−5.50	−4.95	−4.38	−4.12	−3.01	−3.0	−2.37

See text for definitions of D1 to D8.

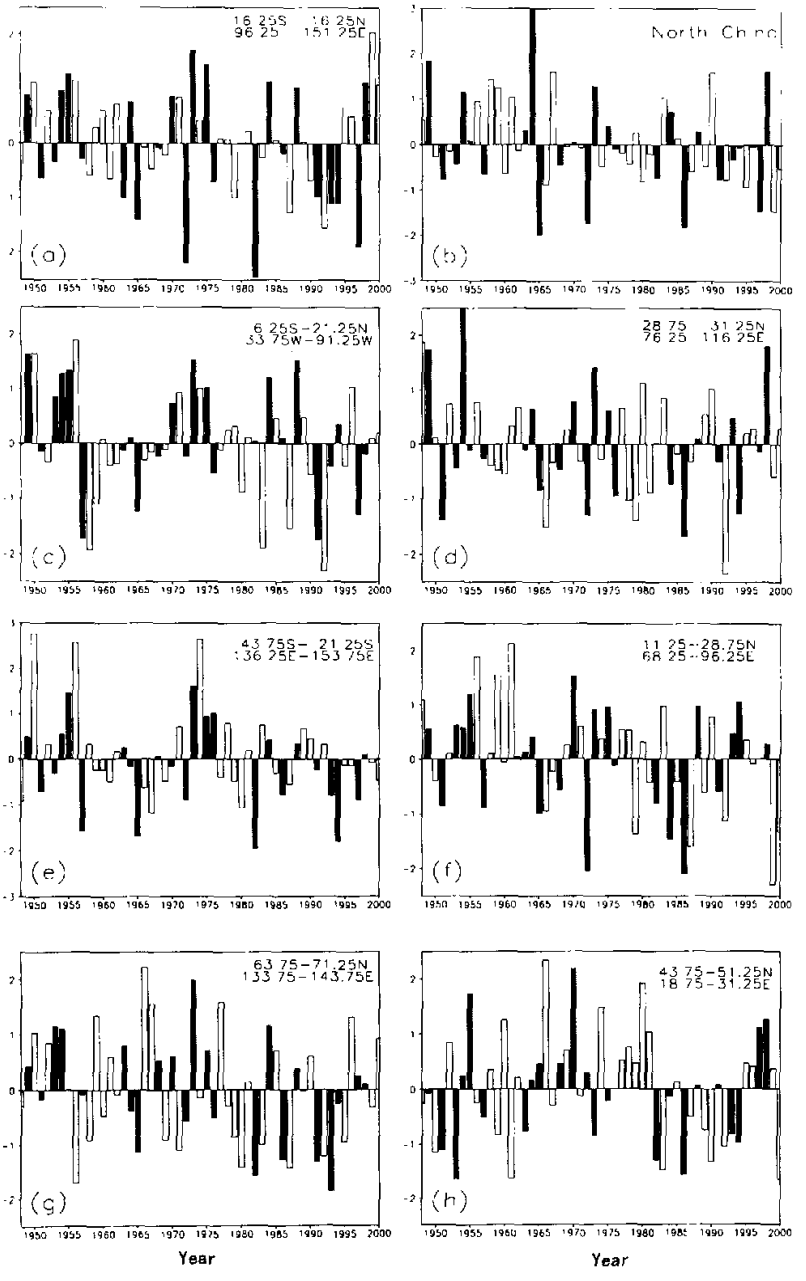

Fig. 2. Temporal variation of the normalized annual rainfall over areas where the annual rainfall is obviously reduced in warm event years. Black (gray) denotes warm (cold) event years.

Table 4. Areas with increased annual rainfall in warm event years and their averaged annual rainfall (Units: mm)

	F1	F2	F3	F4	F5
Warm event	812.2	1242.6	253.5	62.8	1025.0
Cold event	720.5	1121.1	219.9	46.0	980.3
Difference	87.7	121.5	33.6	16.8	44.7
t–Statistic	3.66	3.50	3.20	2.89	1.65

See text for definitions of F1 to F5.

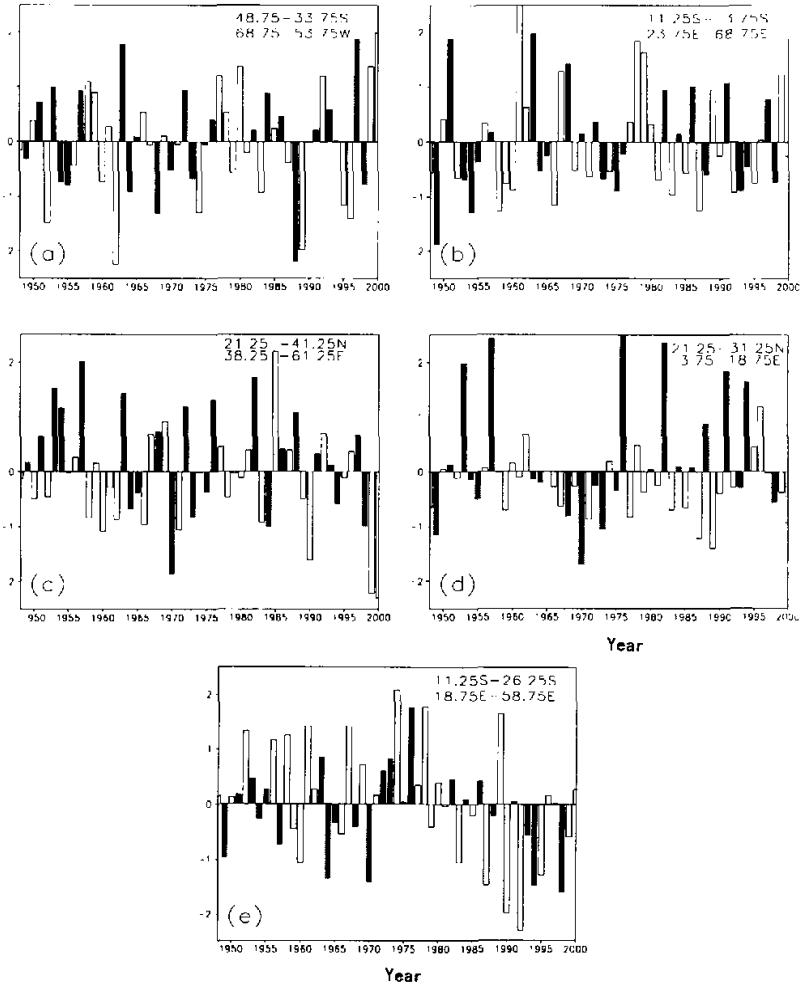

Fig. 3. Temporal variation of the normalized annual rainfall over areas where the annual rainfall is obviously increased in warm event years. Black (gray) denotes warm (cold) event years.

5. Interdecadal anomalies of annual rainfall and ENSO

Many studies show that interdecadal changes have occurred in the atmospheric general circulation since the 1970s. For example, Wang (1994, 1995) pointed out that the ENSO cycle has transitioned from a cold to a warm state. Whether this interdecadal change has affected the global precipitation, is investigated here. ENSO events before and after 1979 were compared and it was found that among the 8 areas D1 to D8, 7 of them were drought areas where the annual rainfall was even less in the warm event years after 1979 than before, and all 8 areas were not waterlogged in the cold event years after 1979. In particular, the mean annual rainfall over the East Australia region (D5) was reduced by 63 mm (41 mm) in warm (cold) event years after 1979 compared with those before, and D1 also underwent a similar change. The mean annual rainfall over D6 was reduced by 150 mm in cold event years after 1979 compared with those before. However, these differences have not reached significance at the 0.05 level. Therefore the interdecadal variations of ENSO have not affected the interdecadal anomalies of the global precipitation, or at least the effect was not detected by the student's t–test performed on the data set used here.

6. Summary and conclusion

The relation between the global land annual precipitation and ENSO during 1948–2000 is investigated using the newly compiled global land monthly precipitation data (PREC / L), and the results of composite analysis are tested with Monte Carlo simulations. It is found that there are 8 significant drought and 5 significant waterlogged areas in the globe during ENSO event years, and we present the drought / waterlogged areas sequenced according to their significance. In warm event years, the land area where the annual rainfall was reduced is far greater than that where the annual rainfall was increased, and the reduction is more significant than the increase. In contrast to the results of previous works, it is pointed out here that North China is a significant area influenced ENSO, by being second in the global name list. The influence of the interdecadal variation of ENSO on the global annual precipitation is insignificant, but the influence of warm events after the 1980s on droughts of East Australia and North China is greater than that before the 1980s. The relation between ENSO and precipitation is complicated. This paper only studies the major variation features of the annual precipitation in the beginning year of ENSO, and of course cannot reveal the time–detailed influence of ENSO on precipitation. Therefore, the results in this paper do not reflect the complete relation between ENSO and global precipitation. It is seemingly necessary to study the relation over seasons or other time periods, and inaddition, using the PREC / O data.

Acknowledgments. The authors would like to thank Dr. M. Y. Chen, P. P. Xie, and J. E. Janowiak of the Climate Prediction Center (NOAA / NWS / NCEP) and PA Arkin of the Office of Global Programs (NOAA / OAR) for providing the global land monthly precipitation data (PREC / L) in this study. This paper was supported by the National Natural Science Foundation of China under Grant No.40275028.

REFERENCES

Bradley, R. S., H. F. Diaz, G. N. Kiladis, and J. K. Eischeid, 1987a: ENSO signal in continental temperature and precipitation records. *Nature*, **327**, 497–500.

Bradley, R. S., H. F. Diaz, J. K. Eischeid, P. D. Jones, P. M. Kelly, C. M. Goodess, 1987b: Precipitation fluctuations over northern hemisphere land areas since the mid-19th century. *Science*, **237**, 171–175.

Chen, M., P. Xie, J. E. Janowiak, P. A. Arkin, 2001: Global Land Precipitation : A 50-yr monthly analysis based on interpolation and reconstruction of gauge observations. *12th Symposium on Global Changes Studies and Climate Variations*. Albuquerque, NM. 14–19 January.

Chen, M., P. Xie, J. E. Janowiak, P. A. Arkin, 2002: Global precipitation: a 50 year monthly analysis based on gauge observations. *Journal of Hydrometeorology*, **3**(3), 249–266.

Hulme, M., 1992: A 1951–80 global land precipitation climatology for the evaluation of general circulation models. *Climate Dynamics*, **7**, 57–72.

Lau, K. M., and P. J. Sheu, 1988: Annual cycle, quasi-biennial oscillation, and Southern Oscillation in global precipitation. *J. Geophys. Res.*, **93**, 10975–10988.

Lau, K. M., and P. J. Sheu, 1991: Teleconnection in global rainfall anomalies: Seasonal to interdecadal time scales. *Teleconnections Linking Worldwide Climate Anomalies*, edited by M. Glantz, R. Katz, and N. Nicholls, Cambridge University Press, Cambridge, U.K.

Li Qingquan, and Ding Yihui, 1997: The basic features of the El Niño events during 1991–1995 and their anomalous influences on the weather and climate in China. *Climatic and Environmental Research*, **2**(2), 163–178 (in Chinese).

Livezey, R. E., and W. Y. Chen, 1983: Statistical field significance and its determination by Monte Carlo techniques. *Mon. Wea. Rev.*, **111**, 46–59.

Nicholson, S. E., B. Some, and B. Kone, 2000: An analysis of recent rainfall conditions in West Africa including the rainy seasons of the 1997 El Niño to 1998 La Niña years. *J. Climate*, **13**, 2628–2640.

Noel, J., and D. Changnon, 1998: A pilot study examining U.S. winter cyclone frequency pattern associated with three ENSO parameters. *J. Climate*, **11**, 2152–2159.

Rasmusson, E. M., and T. H. Carpenter, 1982: Variation in tropical sea surface temperature and surface wind field associated with the Southern Oscillation / El Niño. *Mon. Wea. Rev.*, **110**, 345–384.

Ropelewsi, C. F., and M. S. Halpert, 1987: Global and regional scale precipitation patterns associated with El Niño / Southern Oscillation. *Mon. Wea. Rev.*, **115**, 1606–1626.

Trenberth, K. E., 1997: The definition of El Niño. *Bull. Amer. Meteor. Soc.*, **78**, 2771–1777.

Wang, B., 1994: Transition from a cold to awarm state of the El Niño–Southern Oscillation cycle. *Met. Atmos. Phys.*, **48**, 1–16.

Wang, B., 1995: Interdecadal change in El Niño onset in the last four decades. *J. Climate*, **8**, 267–285.

Wang Shaowu, and Gong Daoyi, 1999: ENSO events and their intensity during the past century. *Meteorological Monthly*, **25**(1), 9–14.

Xu Jianjun, and J. C. L. Chan, 2001: The role of the Asian–Australian monsoon system in the onset time of El Niño. *J. Climate*, **14**, 418–433.

全球陆地年降水量与 ENSO 关系的初步研究

施 能 陈绿文 夏冬冬

摘 要

用全球陆地月降水资料(PREC / L)，研究了 1948–2000 年期间的 ENSO 事件与全球陆地年降水量的关系。对合成分析的结果进行了蒙特卡洛模拟检验。结果表明，暖事件年全球陆地年降水量大范围地明显减少，显著的地区是：赤道西太平洋区，中国的华北，赤道中美洲区，孟加拉湾北部及尼泊尔，东澳大利亚区，印度西部及巴基斯坦南部，勒拿河以东地区，西欧及南极的威尔克斯等区域。在暖事件年，陆地年降水量增加地区不多，主要是南美的智利和阿根廷，

东非索马里，肯尼亚和坦桑尼亚，中东的土耳其、伊拉克及伊朗，北非的利比亚和阿尔及利亚、西南非的纳米比亚及非洲南部的博茨瓦纳和津巴布韦。统计检验表明，暖事件年全球陆地年降水量减少的面积比降水量增加的面积要大，而且更为显著。将本文结果与早期的研究结果进行了比较。研究还指出，ENSO 的年代际变化对上述地区降水的年代际变化影响不明显。但是 80 年代以后的暖事件对东澳大利亚干旱，中国的华北的干旱的影响比 80 年代前的影响更大。

关键词：全球降水，ENSO，全球旱涝，年代际